

Photo-control of the Magnetic Properties of Dy(III) and Ho(III) Homometal Coordination Polymers Bridged by a Diarylethene Ligand

Goulven Cosquer,^{a,b} Masakazu Morimoto,^c Masahiro Irie,^c Ahmed Fetoh,^a Brian K. Breedlove,^{a,b} and Masahiro Yamashita^{*,a,b}

SUPPORTING INFORMATION

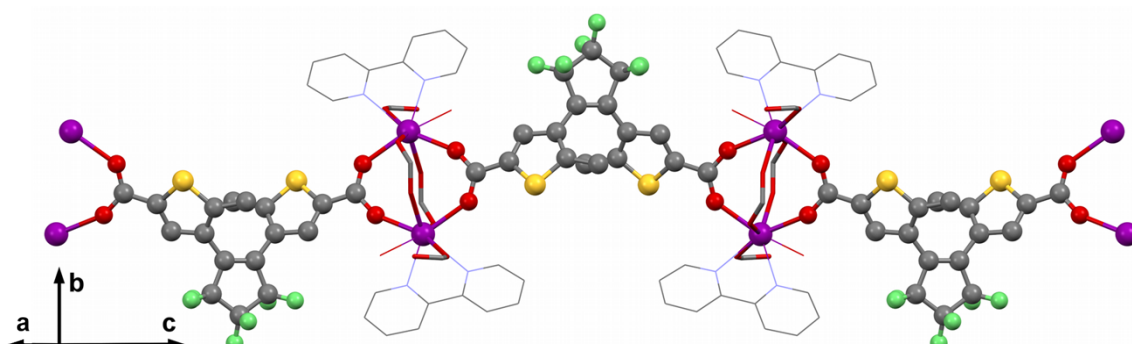


Figure S1. Drawing of the 1D chain in **Dy-o**.

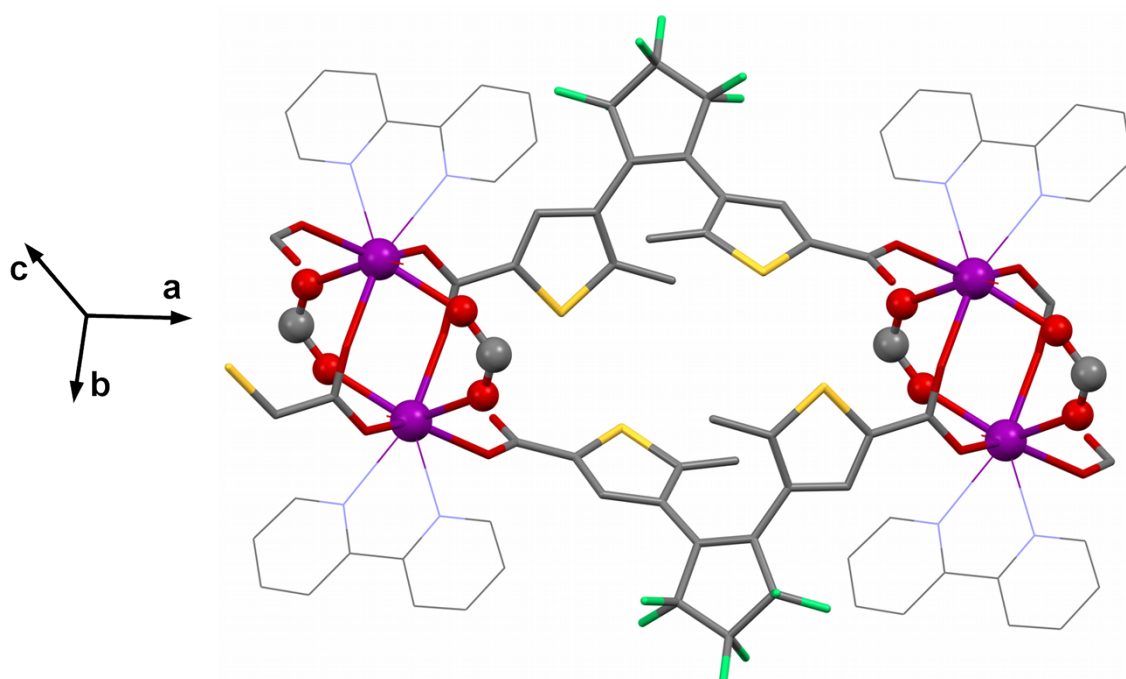


Figure S2. DTE bridges between **Dy-o** 1D chains.

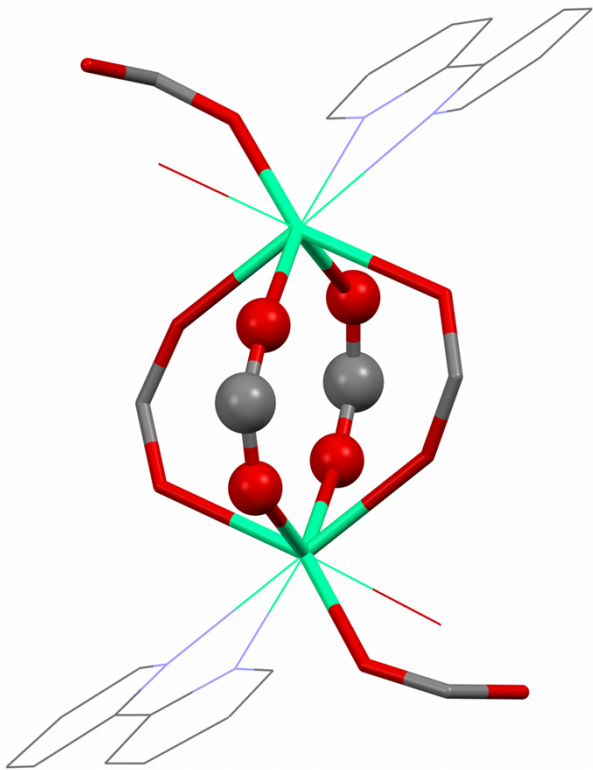


Figure S3. Drawing of the Ho dimer in **Ho-o** with Ho ions and **DTE1** as balls and sticks, **DTE2** and **DTE3** as capped sticks, and bipyridine and water as wires. For clarity, only the carboxylato groups of the DTEs are shown, and the hydrogen atoms are omitted.

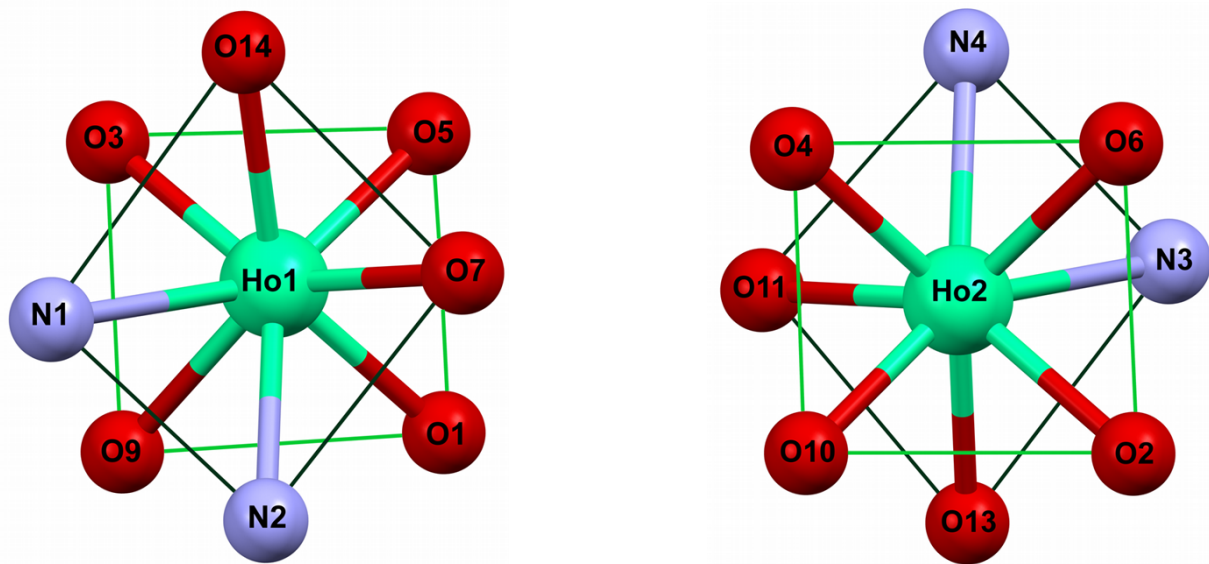


Figure S4. Diagram of the coordination polyhedra in **Ho-o**. The light and dark green lines represent the top and bottom square faces of the antiprism geometry, respectively.

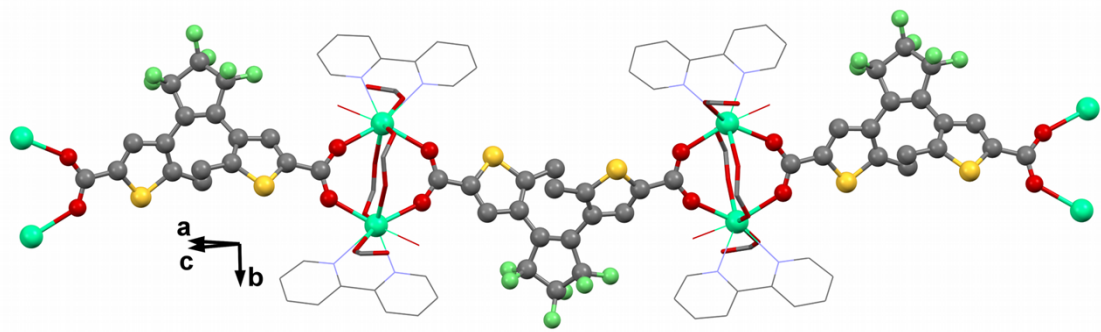


Figure S5. Drawing of the 1D chain of **Ho-o**.

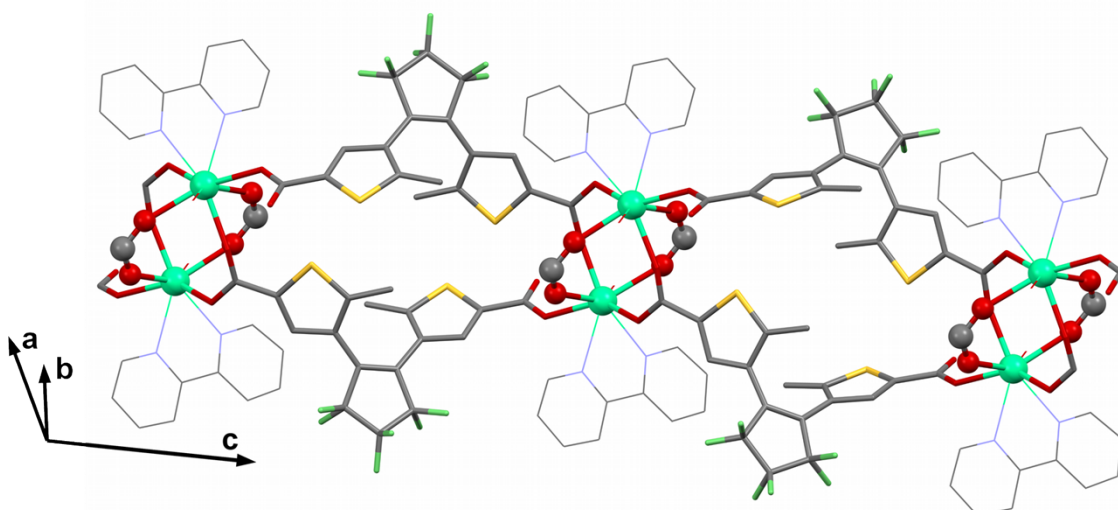


Figure S6. Drawing of intradimer DTE bridges between 1D chains.

Table S1. Parameters obtains from fitting to the extended Debye model for Dy-o without external dc field

Temperature/K	$\chi_{\text{iso}}/\text{cm}^3 \text{ mol}^{-1}$	$\chi_{\text{adia}}/\text{cm}^3 \text{ mol}^{-1}$	α	τ/s
1.85	5.80073	0.46930	0.22490	2.746×10^{-4}
2.00	5.31360	0.45766	0.22232	2.676×10^{-4}
2.15	4.90389	0.41620	0.22268	2.568×10^{-4}
2.30	4.59554	0.42447	0.21962	2.512×10^{-4}
2.45	4.27856	0.42561	0.21811	2.433×10^{-4}
2.60	4.00903	0.42765	0.21715	2.334×10^{-4}
2.75	3.76594	0.40295	0.21872	2.189×10^{-4}
2.90	3.54656	0.39822	0.21870	2.050×10^{-4}

3.05	3.35241	0.42480	0.21705	1.932×10^{-4}
3.20	3.17905	0.43357	0.21763	1.785×10^{-4}
3.35	3.02388	0.44025	0.21695	$1.636e \times 10^{-4}$
3.50	2.88690	0.46835	0.21683	1.510×10^{-4}
4.00	2.50924	0.61412	0.20731	1.182×10^{-4}
4.50	2.21633	0.70989	0.20009	8.900×10^{-5}
5.00	1.98715	0.85778	0.17578	7.179×10^{-5}

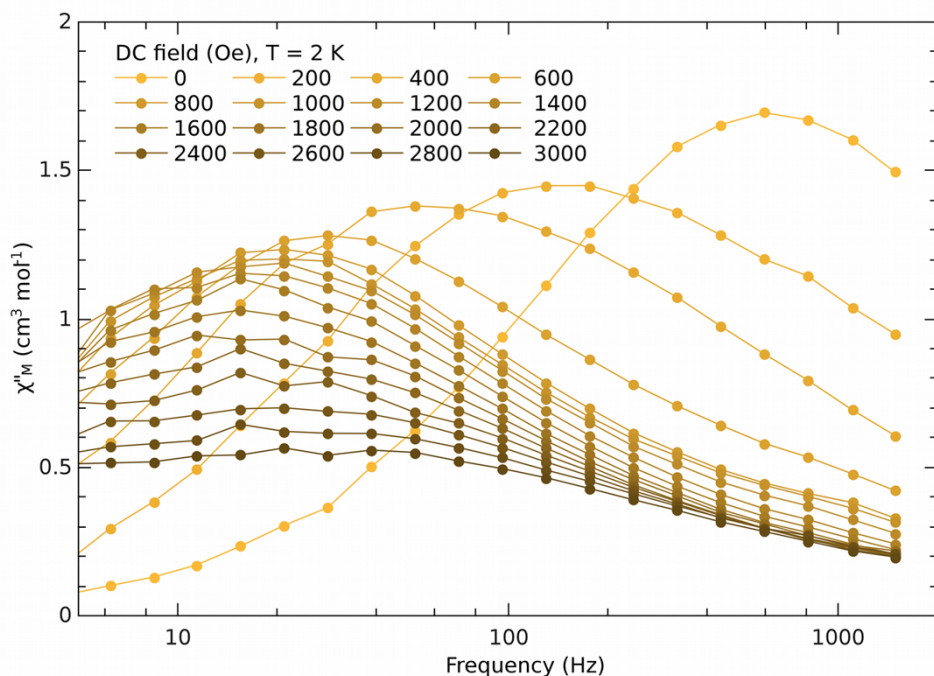


Figure S7. Field dependence of χ_M'' for Dy-0 at 2 K.

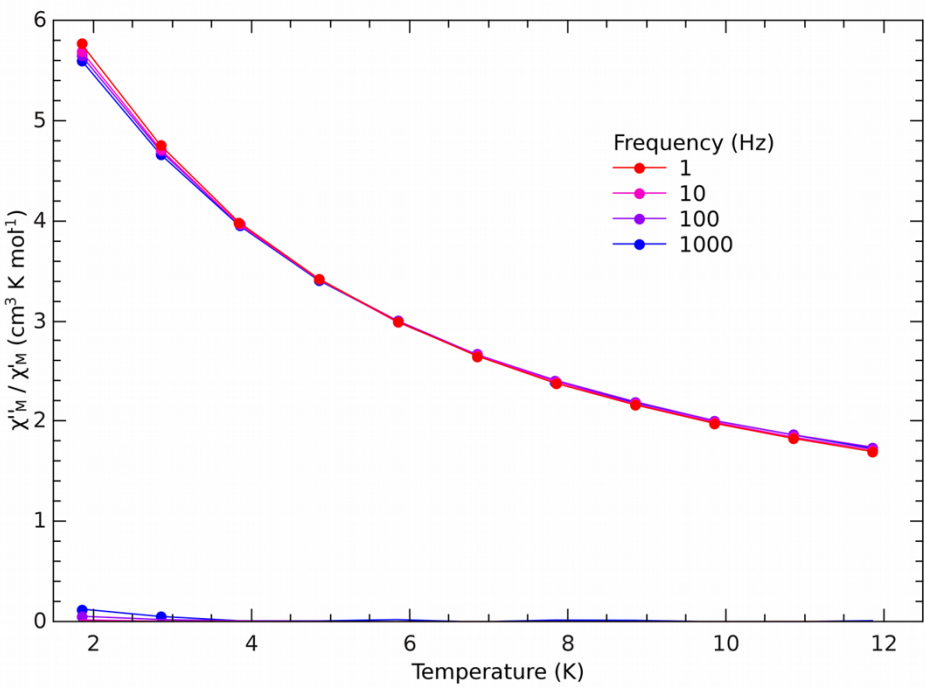


Figure S8. T dependence of χ_M'' and χ_M' for **Ho-o** in a zero dc field.

Table S2: Parameters obtained from fitting to the extended Debye model for Dy-o in an 1000 Oe external dc field

Temperature/K	$\chi_{\text{iso}}/\text{cm}^3 \text{mol}^{-1}$	$\chi_{\text{dia}}/\text{cm}^3 \text{mol}^{-1}$	α	τ/s
1.85	5.36379	0.83990	0.34808	8.936×10^{-3}
2.00	5.04440	0.80308	0.34862	7.669×10^{-3}
2.15	4.81645	0.76841	0.35864	6.556×10^{-3}
2.30	4.47204	0.68151	0.37965	4.899×10^{-3}
2.45	4.16282	0.64965	0.37166	3.452×10^{-3}
2.60	3.88266	0.62158	0.36339	2.468×10^{-3}
2.75	3.66632	0.61599	0.35442	1.844×10^{-3}
2.90	3.44839	0.60106	0.34587	1.324×10^{-3}
3.05	3.25873	0.59559	0.33521	9.644×10^{-4}
3.20	3.11089	0.58822	0.33298	7.160×10^{-4}
3.35	2.92330	0.60259	0.31370	5.205×10^{-4}
3.50	2.81646	0.63649	0.30382	4.100×10^{-4}
4.00	2.45501	0.64062	0.29044	1.623×10^{-4}
4.50	2.18228	0.70507	0.28633	7.562×10^{-5}

5.00	1.96791	0.76468	0.28345	3.904×10^{-5}
------	---------	---------	---------	------------------------

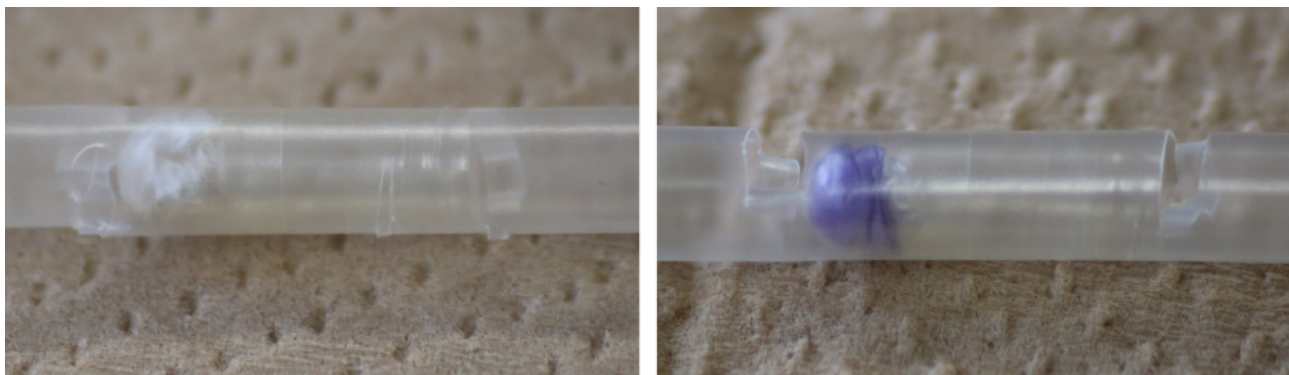


Figure S9. Photographs of the **Dy-o** (left) and **Dy-c** (right) samples used for the magnetic measurements.

Table S3. Parameters obtained from fitting to the extended Debye model for Dy-c in an 1000 Oe external dc field

Temperature/K	$\chi_{\text{iso}}/\text{cm}^3 \text{ mol}^{-1}$	$\chi_{\text{adia}}/\text{cm}^3 \text{ mol}^{-1}$	α	τ/s
1.85	6.07039	0.86860	0.29655	5.244×10^{-3}
2.00	5.63540	0.78490	0.31319	3.937×10^{-3}
2.15	5.26943	0.70319	0.33211	2.879×10^{-3}
2.30	4.99497	0.63943	0.34612	2.178×10^{-3}
2.45	4.70119	0.57814	0.36002	1.568×10^{-3}
2.60	4.43828	0.55796	0.36522	1.169×10^{-3}
2.75	4.22079	0.52088	0.37540	8.774×10^{-4}
2.90	4.00278	0.52829	0.37291	6.714×10^{-4}
3.05	3.80662	0.54522	0.37178	5.257×10^{-4}
3.20	3.62921	0.53656	0.37361	4.047×10^{-4}
3.35	3.46850	0.53527	0.37493	3.166×10^{-4}

3.50	3.32151	0.49156	0.38034	2.382×10^{-4}
4.00	2.91051	0.46506	0.38685	1.057×10^{-4}
4.50	2.58745	0.61729	0.37685	5.990×10^{-5}
5.00	2.32767	0.86635	0.36447	4.366×10^{-5}

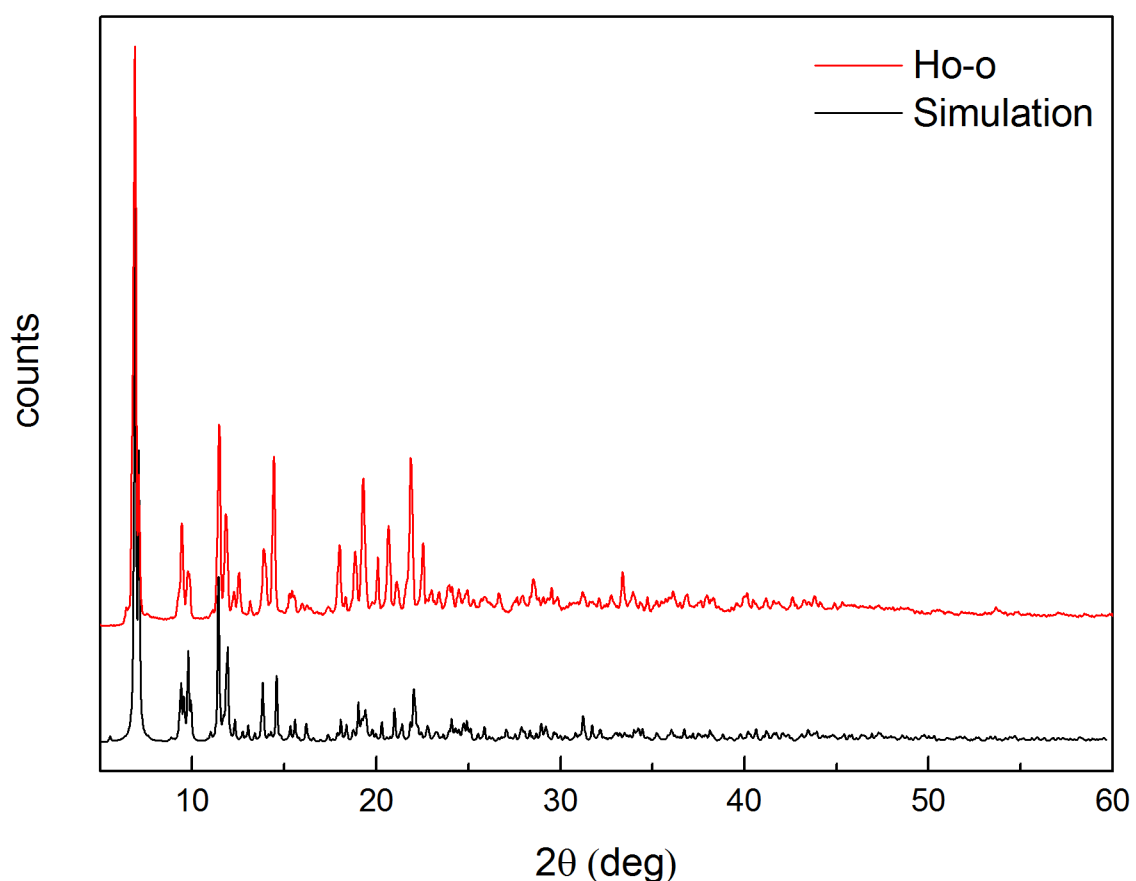


Figure S10. Comparison of the experimental PXRD patterns of **Ho-o** with the simulated single crystal PXRD pattern.

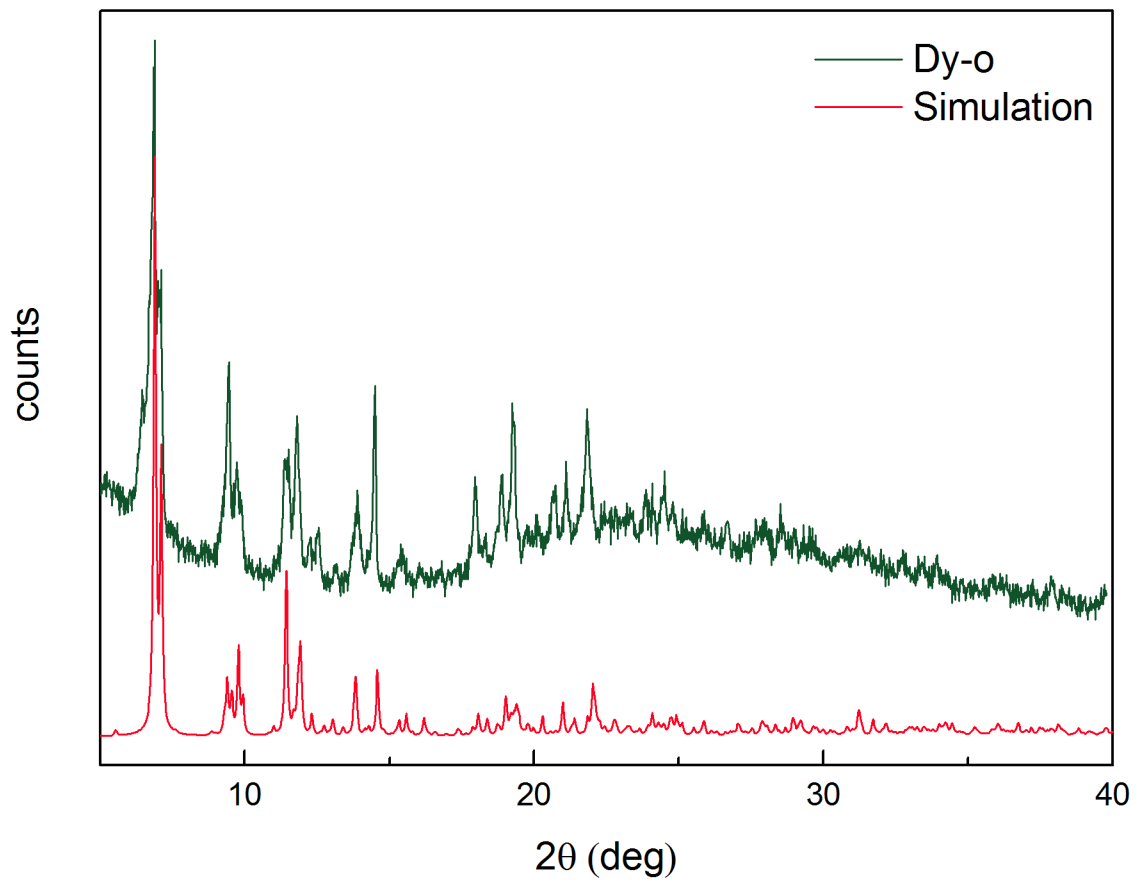


Figure S11. Comparison of the experimental PXRD patterns of **Dy-o** with the simulated single crystal PXRD pattern.